ELSEVIER

Biophysical Chemistry 92 (2001) 155–168

Biophysical Chemistry

www.elsevier.com/locate/bpc

Resonance energy transfer study of peptide–lipid complexes

Galyna Gorbenko[a,*], Hiroyuki Saito[b], Julian Molotkovsky[c], Masafumi Tanaka[d], Masashi Egashira[d], Minoru Nakano[d], Tetsurou Handa[a]

[a] *Kharkov National University, Department of Physics and Technology, 4 Svoboda Sq., Kharkov, 61077, Ukraine*
[b] *Osaka Branch National Institute of Health Sciences, Osaka 540-0006, Japan*
[c] *Shemyakin-Ovchinnikov Institute of Bioorganic Chemistry, Russian Academy of Sciences, 16 / 10 Miklukho-Maklaya, Moscow, 117871, Russia*
[d] *Graduate School of Pharmaceutical Sciences, Kyoto University, Sakyo-ku, Kyoto 606-8501, Japan*

Received 3 April 2001; received in revised form 26 June 2001; accepted 4 July 2001

Abstract

Resonance energy transfer involving tryptophan as a donor and anthrylvinyl-labeled phosphatidylcholine (AV-PC), 3-methoxybenzanthrone (MBA) and 8-anilino-1-naphthalene sulfonic acid (ANS) as acceptors has been examined to obtain information on the structure of peptide–lipid systems consisting of 18A or Ac-18A-NH_2 peptides and large unilamellar phosphatidylcholine vesicles. The lower and upper limits for the tryptophan distance from the bilayer midplane have been assessed in terms of the models of energy transfer in two-dimensional systems, taking into account orientational effects. Evidence for the existence of preferential orientations of Ac-18A-NH_2 with respect to the lipid–water interface has been obtained.

Keywords: Resonance energy transfer; 18A peptides; Phosphatidylcholine vesicles; Bilayer location of tryptophan

1. Introduction

Resonance energy transfer (RET) has long been used in elucidating the mechanisms of a wide variety of processes occurring in natural and model membranes including molecular clustering, binding, aggregation and exchange phenomena [1–4]. Since a principal feature of energy transfer consists in its dependence on the distance between donor and acceptor, a major part of RET studies are aimed at structural characterization of membrane systems [5,6]. To derive the most valid quantitative information from the RET measurements one should take into account such factors as the curvature of the lipid–water interface, mutual disposition of donors and acceptors in the

* Corresponding author. 52-52 Tobolskaya Str., Kharkov, 61072, Ukraine.

0301-4622/01/$ - see front matter
PII: S0301-4622(01)00195-8

outer and inner bilayer leaflets, the randomness of acceptor distribution in two dimensions, the effect of excluded area, etc. The role of these factors in determining the extent of energy transfer has been analyzed in a number of theoretical models [7–9]. One of such models, developed by Wolber and Hudson [10] for donors and acceptors randomly distributed in a plane, has been modified in the present study in examining energy transfer from the peptide tryptophan residue as a donor to fluorescent probes located in the lipid phase as acceptors. Our main goal was to evaluate the tryptophan location in the complexes of Ac-18A-NH_2 and 18A peptides with large unilamellar lipid vesicles (LUV) composed of phosphatidylcholine (PC). In approaching this goal, we have extended the model of Wolber and Hudson to the case of one donor and two acceptor planes and have suggested some approaches to reducing the limitations of RET method, in particular, those caused by uncertainty in the orientation factor value [11]. These approaches involve simultaneous analysis of the results obtained with different acceptors and varying the value of orientation factor in the data fitting.

Class A amphipathic peptides 18A and Ac-18A-NH_2 chosen for our study are now extensively used in modeling the lipid-binding site of apolipoprotein A–I and other exchangeable apolipoproteins [12,13]. These peptides have identical amino acid sequences (Asp–Trp–Leu–Lys–Ala–Phe–Tyr–Asp–Lys–Val–Ala–Glu–Lys–Leu–Lys–Glu–Ala–Phe) but helicity of Ac-18A-NH_2 is several fold higher than that of 18A, both in the free and lipid-bound state [14]. Such a difference in the secondary structure is thought to originate from the removal of repulsive electrostatic interactions between the peptide dipole and the ends of polypeptide chain by attaching a carbonyl at the amino terminus and an amide at the carboxyl terminus. According to the helical wheel representation of 18A and Ac-18A-NH_2 peptides, positively charged Lys residues are located at the polar–non-polar interface of the amphipathic α-helix, while negatively charged Asp and Glu reside at the center of the polar face [15]. It has been suggested that high lipid affinity of the class A α-helices stems from the snorkeling of the basic residues with significant hydrophobicity, particularly, lysine and arginine toward the polar helix face, with their charged groups being located in the aqueous phase and hydrocarbon side chain penetrating in the hydrophobic bilayer region [16]. It is generally assumed that class A amphipathic peptides adopt parallel to the membrane surface orientation providing thermodynamically favorable contacts between the polar and non-polar parts of the α-helix and lipid bilayer. Evidence for such an orientation has been provided by the 'fluorescence footprinting' [17] (18A) and X-ray diffraction studies [18] (Ac-18A-NH_2). Assuming parallel to the membrane surface disposition of 18A and Ac-18A-NH_2 a single tryptophan residue localized at the hydrophilic helix face near the polar–non-polar boundary could be expected to reside in the polar bilayer region. Such a location has been suggested by Clayton and Sawyer for 18A Trp [17], while for Ac-18A-NH_2 the position of the tryptophan residue is not yet unequivocally ascertained. Meanwhile, widespread assumption about matching between the polar and non-polar parts of the peptide and phospholipid molecules seems to be rather simplified so that elucidating the factors responsible for the disposition of the amphipathic α-helix in the lipid bilayer requires characterization of the bilayer penetration of individual amino acids and systematization of the findings derived for a great number of peptides by a variety of techniques. In view of this in the present work it seemed reasonable to address the question concerning the localization of the 18A and Ac-18A-NH_2 tryptophan residues in the lipid-bound state. In addition, by examining model systems with a certain helix disposition it was of interest to test the validity of the approach proposed in our previous studies for determining specific protein or peptide orientation with respect to the lipid–water interface on the basis of RET measurements [19,20].

2. Materials and methods

2.1. Chemicals

Egg yolk PC was kindly provided by Asahi

Kasei Co. (Japan). The phospholipid purity assessed by thin layer chromatography exceeds 99.5%. 18A and Ac-18A-NH_2 peptides were purchased from Takara Shuzo Co. (Japan). The high performance liquid chromatography, amino acid analysis and mass spectrometry indicated purity above 98% for both peptides. MBA and ANS were purchased from Zonde (Latvia). AV-PC was synthesized as described in detail elsewhere [21]. All other chemicals were of special grade from Wako Pure Chemicals (Japan).

2.2. Preparation of lipid vesicles

Large unilamellar vesicles (LUV) were prepared from PC by the extrusion method. A thin PC film obtained by evaporation of its chloroform solution was left under vacuum overnight to remove residual organic solvent, and was subsequently hydrated with 10 mM Tris–HCl buffer, pH 7.4, containing 1 mM EDTA. After subjecting to five freeze–thaw cycles lipid suspension was extruded through a 100-nm pore size polycarbonate filter. Phospholipid concentration was determined according to the procedure of Bartlett [22].

In the RET experiments, solutions of PC and acceptors (AV-PC or MBA) in organic solvents were mixed prior to the vesicle preparation. Concentrations of MBA and AV-PC in the lipid bilayer were determined spectrophotometrically, after 10-fold dilution of the vesicle suspension by ethanol. When ANS was used as acceptor, the aliquots of the probe solution in buffer were added to the preformed LUVs. A separate series of experiments was performed for evaluation of the binding parameters characterizing the ANS–lipid complexes with subsequent calculation of the concentration of membrane-bound probe.

2.3. Resonance energy transfer measurements

Fluorescence measurements were performed with a HITACHI F-4500 spectrofluorimeter using a 5-mm path-length cuvette. Peptide emission spectra were recorded at 25°C with 296-nm excitation wavelength. Excitation and emission slit widths were set at 5 nm. The quantum yield of the peptide tryptophan (Q_p) was estimated using tryptophan solution in water as a standard (Q_s = 0.14 [23]), according to the relationship:

$$Q_p = \frac{Q_s\left(1 - 10^{-A}|S_p\right)}{(1 - 10^{-A_p})S_s} \quad (1)$$

where A is the absorbance at the excitation wavelength, S is the total area under emission spectrum, subscripts 's' and 'p' correspond to standard and peptide, respectively.

The RET efficiency was estimated through determining the ratio of the Trp quantum yields in the absence (Q_D) and presence (Q_{DA}) of acceptors ($E = 1 - Q_{DA}/Q_D$). This method of RET measurements generally makes for a higher accuracy of E value compared to that ensured by monitoring the sensitized acceptor emission [1]. The measured fluorescence intensities of a donor were corrected for the inner filter and reabsorption effects using the following coefficients:

$$k = \frac{(1 - 10^{-A_o})(A_o + A_a)}{(1 - 10^{-(A_o + A_a)})A_o} \quad (2)$$

where A_o is the peptide absorbance in the absence of acceptor ($A_o \sim 0.02$), A_a is the acceptor absorbance at the excitation or emission wavelengths. The acceptors being utilized include ANS, localizing at the outer membrane side, MBA and AV-PC distributing between the outer and inner bilayer leaflets. The employed acceptor concentrations were chosen from the range 5.5–25 μM for AV-PC; 2.5–10 μM for MBA and 1.7–17 μM for ANS. At the excitation wavelength the maximum acceptor concentrations correspond to the following A_a values: 0.016 (AV-PC); 0.09 (MBA); 0.01 (ANS). Analogous values derived for the maximum of the donor emission spectrum (333 nm and 342 nm for the lipid-bound Ac-18A-NH_2 and 18A, respectively) fall in the range 0.05–0.07 for AV-PC; 0.03–0.05 for MBA and 0.05–0.08 for ANS.

The critical distance of energy transfer (Förster radius, nm) was calculated as [1]:

$$R_o = 979(\kappa^2 n_r^{-4} Q_D J)^{1/6} \quad (3)$$

$$J = \frac{\int_0^\infty F_D(\lambda)\varepsilon_A(\lambda)\lambda^4 d\lambda}{\int_0^\infty F_D(\lambda)d\lambda} \quad (4)$$

where Q_D is the donor quantum yield, n_r is the refractive index of the medium ($n_r = 1.37$), κ^2 is an orientation factor, J is the overlap integral calculated by the numerical integration, $F_D(\lambda)$ is the donor fluorescence intensity, and ε_A (λ) is the acceptor molar absorbance at the wavelength λ.

To obtain the most adequate information on the structure of peptide–lipid systems, the results of energy transfer measurements were analyzed in terms of the modified model of Wolber and Hudson [10], developed for the case of the random two-dimensional distribution of donors and acceptors. Since acceptors employed in the present study differ in their partitioning in the lipid bilayer, the following two cases have been considered: (i) donor and acceptor planar arrays are situated in the outer monolayer; and (ii) acceptors are uniformly distributed between the outer and inner bilayer leaflets while donors reside only at the outer membrane side. In the former case, relative quantum yield of a donor (Q_r) is given by:

$$Q_r = \frac{Q_{DA}}{Q_D} = \int_0^\infty \exp[-\lambda](I(\lambda))^N d\lambda \quad (5)$$

$$I(\lambda) = \int_{d_a}^{R_d} \exp\left[-\lambda(R_o/R)^6\right] W(R) dR \quad (6)$$

$$N = \pi R_d^2 C_a^s; \quad W(R) = \frac{2R}{R_d^2 - d_a^2} \quad (7)$$

where $\lambda = t/\tau_d$, τ_d is the lifetime of an excited donor in the absence of acceptor; $W(R)dR$ is the probability of finding acceptors in the annulus between radii R and $R + dR$; N is the number of acceptors within the disc of radius R_d, beyond which energy transfer is insignificant; C_a^s is the acceptor concentration per unit area; d_a is the separation of the donor and acceptor planes. In the latter of the aforementioned cases a Q_r value is represented as a sum of two contributions, describing energy transfer to the acceptor arrays localized in the outer and inner bilayer leaflets [20]:

$$Q_r = 0.5\left(\int_0^\infty \exp[-\lambda](I_1(\lambda))^{N_1} d\lambda + \int_0^\infty \exp[-\lambda](I_2(\lambda))^{N_2} d\lambda\right) \quad (8)$$

$$I_1(\lambda) = \int_{d_a}^{R_d} \exp\left[-\lambda(R_o/R)^6\right]\left(\frac{2R}{R_d^2 - d_a^2}\right) dR \quad (9)$$

$$I_2(\lambda) = \int_{d_t \pm d_a}^{R_d} \exp\left[-\lambda(R_o/R)^6\right] \times \left(\frac{2R}{R_d^2 - (d_t \pm d_a)^2}\right) dR \quad (10)$$

$$N_1 = \pi C_a^s (R_d^2 - d_a^2);$$
$$N_2 = \pi C_a^s \left(R_d^2 - (d_t \pm d_a)^2\right) \quad (11)$$

where d_t is the separation of acceptor planes, localized at the outer and inner membrane sides, sign '+' corresponds to the case when acceptors in the outer monolayer are situated deeper than donors, while sign '−' characterizes the opposite case.

3. Results

3.1. Characterization of donors and acceptors

To derive reliable structural information on the basis of RET measurements it is desirable to compare the results obtained for several donor–acceptor pairs. As indicated above, in the present study the peptide tryptophan served as an energy donor with a series of lipid-bound fluorescent probes being the acceptors. Since the peptides under investigation contain two intrinsic fluorophores (Trp and Tyr) that could act as the

energy donors, it seems of importance to perform RET measurements under the conditions allowing unequivocal interpretation of the experimental data. To ensure predominant contribution of tryptophan to the peptide emission spectra the fluorescence was excited at 296 nm. This wavelength is conducive to the selective excitation of tryptophan because its extinction coefficient ($E_{296} \sim 1.5 \times 10^3$ M^{-1} cm^{-1}) is significantly greater than that of tyrosine ($E_{296} \sim 30$ M^{-1} cm^{-1}) [1]. It is also noteworthy that tryptophan fluorescence is known to be much more sensitive to the fluorophore local environment compared to that of tyrosine [1]. According to our observations, association of the peptides with the lipid vesicles was accompanied by a considerable blue shift of the emission maximum (~ 10 nm for 18A and ~ 16 nm for Ac-18A-NH_2) coupled with the increase in the fluorescence intensity. Such pronounced spectral changes strongly suggest that the measured emission spectra are primarily determined by tryptophan, with the tyrosine contribution being negligibly small. All the above arguments allowed us to consider the peptide tryptophan as the only energy donor.

The acceptors being used differ in their structure and localization in the lipid bilayer (Fig. 1). ANS, bearing a negative charge at neutral pH, is known to reside in the polar membrane part [24]. Hydrophobic probe MBA is situated in the glycerol backbone region, partitioning between the outer and inner bilayer leaflets [25], while anthrylvinyl fluorophore of the AV-PC probe is localized in the vicinity of terminal methyl groups of the lipid acyl chains [21]. Fig. 2 illustrates the arrangement of the donor and acceptor planar arrays in the lipid bilayer. MBA and AV-PC are assumed to be uniformly distributed between the outer and inner monolayers, whereas ANS is presumably located at the outer membrane side. Peptide tryptophan which acts as an energy donor is supposed to reside in the outer bilayer leaflets because, to our knowledge, there exists no evidence for the translocation of the 18A or blocked 18A across the membrane.

Since AV-PC and MBA were mixed with PC before the vesicle formation all the probe molecules appeared to be incorporated in the lipid bilayer. Meanwhile, in the case of a water-soluble probe ANS being added to the preformed liposomes, correct application of the aforementioned energy transfer models requires knowing the surface acceptor concentration (C_a^s) related to the molar concentration of the membrane-bound probe (B_z). The value of B_z were estimated using the method of double fluorimetric titration [25]. It was assumed that increase of the ANS fluorescence intensity observed at the probe binding to lipids (ΔI_z) is proportional to the concentration of bound ANS:

$$\Delta I_z = a_z B_z \tag{12}$$

where a_z is a coefficient of proportionality. If the probe binding site contains n_z lipid molecules, the association constant (K_z) can be written as:

$$K_z = \frac{B_z}{F_z(L_o/n_z - B_z)} \tag{13}$$

where F_z is the concentration of free probe, L_o is the total lipid concentration. By combining Eqs. (12) and (13) one obtains the following expression for the total probe concentration (Z_o):

$$Z_o = B_z + F_z = \Delta I_z \left(\frac{1}{a_z} + \frac{n_z}{K_z(L_o a_z - n_z \Delta I_z)} \right) \tag{14}$$

To evaluate K_z, n_z and a_z, we employed nonlinear fitting involving comparison of Z_o values calculated from Eq. (14) with those determined spectrophotometrically, using extinction coefficient $E_{350} = 5.6 \times 10^3$ M^{-1} cm^{-1} [25]. Initial estimates of the binding parameters were obtained from the double reciprocal plots based on the following approximations. In the case when $Z_o \gg B_z$ Eqs. (13) and (14) can be rearranged to give:

$$\frac{1}{\Delta I_z} = \frac{n_z}{a_z L_o} + \frac{n_z}{a_z K_z L_o Z_o} \tag{15}$$

The x-intercept of the plot of $1/\Delta I_z$ vs. $1/Z_o$ yields K_z, while the y-intercept gives the value of $n_z/L_o a_z$. The dependencies $1/\Delta I_z$ ($1/Z_o$) were derived from the results of vesicle titration by the

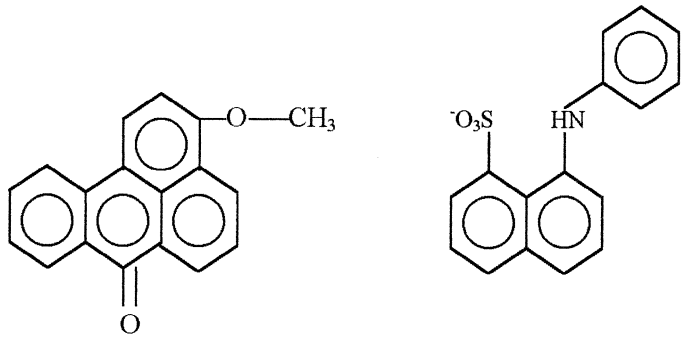

3-methoxybenzanthrone (MBA)

8-anilino-1-naphthalene sulfonic acid (ANS)

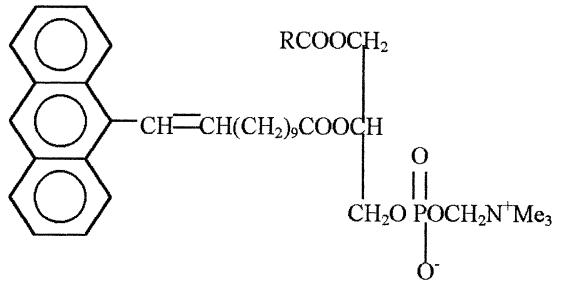

Anthrylvinyl-labeled phosphatidylcholine (AV-PC)

Fig. 1. Structures of the fluorescent probes employed as acceptors in the RET measurements.

probe. By considering the case when $L_o/n_z \gg B_z$, from Eqs. (13) and (14) it follows:

$$\frac{1}{\Delta I_z} = \frac{1}{a_z Z_o} + \frac{n_z}{a_z K_z Z_o L_o} \tag{16}$$

The y-intercept of the $1/\Delta I_z$ plot vs. $1/L_o$ equals $1/Z_o a_z$ thus yielding an approximate value of a_z. To obtain the plots $1/\Delta I_z$ $(1/L_o)$, the probe was titrated by liposomes.

Using this approach the parameters of ANS binding to lipids were estimated to be: $K_z = (5.4 \pm 1.1) \times 10^5$ M^{-1}; $n_z = 41 \pm 7$; $a_z = (8.6 \pm 1.7) \times 10^7$ M^{-1}. These values were used for calculating the concentration of lipid-bound probe according to the relationship stemming from Eq. (13):

$$B_z = 0.5\Big[Z_o + L_o/n_z + 1/K_z - \sqrt{(Z_o + L_o/n_z + 1/K_z)^2 - 4Z_o L_o/n_z}\Big] \tag{17}$$

The surface acceptor concentration was determined as follows:

$$C_a^s = \frac{B_z}{L_o S_{PC}} \tag{18}$$

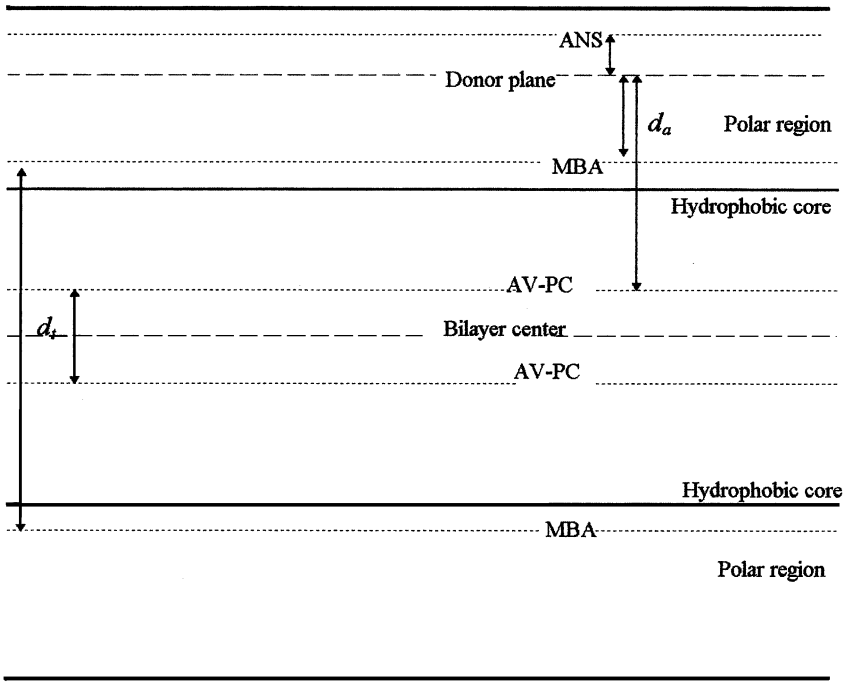

Fig. 2. Schematic representation of the location of donor and acceptor planar arrays in the lipid bilayer.

where S_{PC} is the mean surface area of PC, taken to be 0.65 nm^2 [26]. Note that in the case of ANS C_a^s was calculated using $L_o/2$ instead of L_o. The C_a^s value multiplied by R_o^2 yields the number of acceptors per R_o^2, parameter, commonly employed in the energy transfer studies of two-dimensional systems [7–9].

3.2. Resonance energy transfer studies

Shown in Fig. 3 are the plots of the relative quantum yield of the peptide tryptophan vs. surface acceptor concentration. The experimental Q_r values Q_r^e were fitted to those calculated in terms of the aforementioned models (Q_r^t) by the numerical integration of Eq. (5) or Eq. (8). The fitting procedure was based on the minimization of the function:

$$f = \frac{1}{n_a} \sum_{i=1}^{n_a} (Q_r^e - Q_r^t)^2 \qquad (19)$$

where n_a is the number of acceptor concentrations employed in the RET measurements. The f values derived in the data treatment range between 9×10^{-5} and 6×10^{-4}.

In analyzing the results obtained with ANS, energy transfer between the donor and acceptor planar arrays localized in the outer monolayer was described by Eqs. (5)–(7), while in the cases of MBA and AV-PC distributed between both membrane leaflets, experimental dependencies $Q_r(C_a^s)$ were fitted to Eqs. (8)–(11). The data fitting involved optimization of the parameter d_a at the constant values of d_t and κ^2. Given the dimensions of the PC bilayer [26] and aforementioned assumptions concerning the probe bilayer location, parameter d_t characterizing the separation between the outer and inner acceptor planes was chosen from the range 2.4–2.6 nm for MBA, and 0.2–0.3 nm for AV-PC. It should be noted that due to the high mobility of the terminal groups of acyl chains anthrylvinyl fluorophores could, in principle, be regarded as residing at the

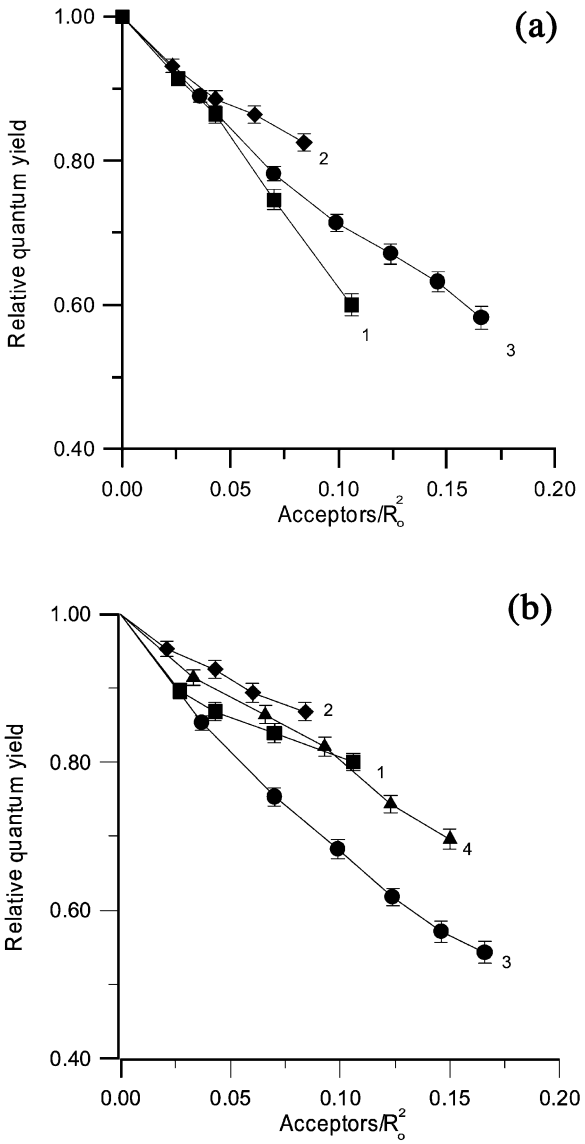

Fig. 3. Relative quantum yield of the donors vs. surface acceptor concentration. Donors: A-Ac-18A-NH_2; B-18A Trp (curves 1–3), ANS (curve 4). Acceptors: 1-AV-PC; 2,4-MBA; 3-ANS.

bilayer midplane. Formally, in the data treatment we consider the two acceptor planes, but the distance between these planes proved to be too small to provide a marked difference between the Q_r contributions calculated from Eqs. (9) and (10). Therefore, considering the only acceptor plane instead of the two ones does not considerably affect the quantitative interpretation of the data derived with AV-PC.

The sets of parameters (d_a, d_t) providing the best fit of experimental data obtained with MBA and AV-PC were subsequently used for calculating the tryptophan distance from the bilayer midplane (d_c) according to the relationship:

$$d_c = 0.5d_t \pm d_a \quad (20)$$

where '+' stands for the location of the outer acceptor plane deeper than the donor plane, while '−' corresponds to the opposite case.

To derive analogous estimates from the results of RET measurements performed with ANS we employed the following approach. Firstly, by examining the energy transfer between ANS as a donor and MBA as an acceptor ($R_o = 3.24$ nm) the separation between the planar arrays of these probes was determined within the framework of the model described by Eqs. (5)–(7). Secondly, ANS distance from the bilayer center (d_{ca}) was calculated from Eq. (20). By analyzing experimental dependencies $Q_r(C_a^s)$ presented in Fig. 3b (curve 4) the value of d_{ca} was estimated to be 1.7 nm. Thirdly, the model describing energy transfer between the donors and acceptors positioned in the outer monolayer [Eqs. (5)–(7)] was applied to evaluating the separation of the Trp and ANS planes (d_{at}). Ultimately, the Trp distance from the bilayer center was calculated as follows:

$$d_c = d_{ca} + d_{at} \quad (21)$$

provided that Trp is located closer to the bilayer surface than ANS and

$$d_c = d_{ca} - d_{at} \quad (22)$$

in the opposite case. Eq. (21) was used in determining the d_c value for the 18A-lipid system assuming that ANS is buried deeper in the membrane interior than Trp. The validity of such an assumption comes from the finding that the emission maximum of the 18A Trp (342 nm) is characteristic of the fluorophore residing in the headgroup region of the lipid bilayer [17]. Meanwhile, the emission maximum of the Ac-18A-NH_2 (333

nm) suggests rather deep penetration of the Trp residue in the membrane interior [27], so that in this case the d_c estimate was derived from Eq. (22).

It seems of significance to note the model described by Eqs. (4)–(10) does not consider the possibility of excluding a certain area at the acceptor plane due to penetration of the relatively large peptide molecule to the level of acceptor disposition. This may particularly be the case for ANS and MBA residing at the lipid–water interface, since the peptide α-helix cylinder lying parallel to the membrane surface has a diameter of approximately 1 nm [28] that is comparable with the size of the headgroup bilayer region. One way to take into account the effect of excluded area is based on introducing a distance of lateral separation between donor and acceptor (R_e) into Eqs. (6) and (9) [19], and taking the lower integration limit to be $R_{min} = \sqrt{d_a^2 + R_e^2}$:

$$I_1(\lambda) = \int_{R_{min}}^{R_d} \exp\left[-\lambda(R_o/R)^6\right] \times \left(\frac{2R}{R_d^2 - d_a^2 - R_e^2}\right) dR;$$

$$N_1 = \pi C_a^s (R_d^2 - d_a^2 - R_e^2) \quad (23)$$

Given that the α-helix cylinder of the 18A peptides under study has a length of approximately 2.7 nm [28], the values of R_e are likely to range from 1 to 3 nm. The data treatment in terms of Eq. (23) with R_e being varied in the above limits yields the maximum d_c values more than twofold smaller compared to those presented in Fig. 4 ($R_e = 0$). Since our model [Eq. (23)] provides a very simplified approach to the problem of excluded area, in interpreting the experimental data it seemed reasonable to consider the widest d_c limits recovered for the case where $R_e = 0$.

Of particular importance in analyzing the results of RET measurements is the question concerning the choice of the orientation factor value used in the calculation of Förster radius [Eq. (3), Table 1]. This factor, depending on the angle between the donor emission and acceptor

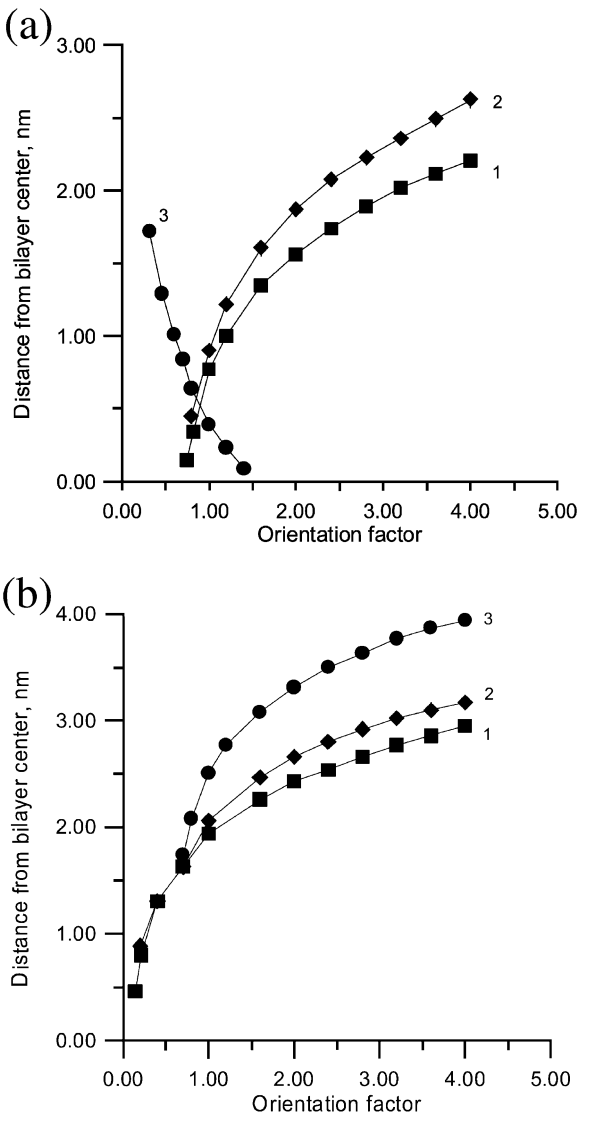

Fig. 4. The distance of Ac-18A-NH_2 (a) and 18A (b) tryptophan residues from the lipid bilayer center as a function of orientation factor. Acceptors: 1-AV-PC; 2-MBA; 3-ANS.

absorption transition dipoles, and the angles between these dipoles and a vector joining donor and acceptor, can change from 0 to 4, the minimum value corresponds to perpendicularly oriented donor and acceptor dipoles, while the maximum one characterizes the case when these dipoles are parallel and identically directed [1]. In the most RET studies κ^2 is taken as 0.67, the

Table 1
Critical distances of energy transfer

Acceptor	Förster radius calculated from Eq. (2) with $\kappa^2 = 0.67$, nm	
	Ac-18A-NH_2	18A
AV-PC	2.23	2.25
MBA	1.88	1.86
ANS	2.22	2.21

value that is valid for the isotropic and dynamic averaging conditions when donors and acceptors are rapidly tumbling and their transition dipoles can adopt all orientations in a short time compared with the transfer time [11]. However, in the membranes which are known to be highly anisotropic systems, fluorophores usually have limited freedom of motion, and the isotropic condition is hardly satisfied. In addition, if there exist certain preferable orientations of the donor and acceptor dipoles, κ^2 value may substantially differ from that in the isotropic conditions. Such an uncertainty in the choice of orientation factor may lead to considerable ambiguities in the data interpretation, especially in the case when the true value of this parameter is less than 1. Unfortunately, because of substantial difficulties in obtaining reliable crystallographic or spectroscopic information on the fluorophore orientation in the lipid bilayer, any accurate assessment of κ^2 appears to be impossible. In view of this we have found it reasonable to chose κ^2 from the widest range (0–4). As has been shown in our previous works [19,20], varying the value of κ^2 in the data fitting and subsequent analysis of the dependencies $d_c(\kappa^2)$ can, in some cases, provide evidence for specific orientation of the fluorophore with respect to the bilayer surface. Taking into account all the aforementioned reasons, the treatment of the results of RET measurements presented here was aimed at obtaining the sets of parameters (d_a, d_t, κ^2) with subsequent analysis of the dependencies $d_c(\kappa^2)$.

4. Discussion

Shown in Fig. 4 are the relationships between the Trp distance from the bilayer center and orientation factor. As can be seen, for each of the acceptors used there exists a certain minimum κ^2 value corresponding to the x-intercept of the plots $d_c(\kappa^2)$ ($d_c = 0$). It appeared that for the donor–acceptor pairs containing Ac-18A-NH_2 Trp as a donor and AV-PC or MBA as acceptors the lower κ^2 limit derived from the data fitting is larger than the isotropic value (0.67). This observation strongly suggests that rotational mobility of the Ac-18A-NH_2 Trp in the lipid-bound state is considerably restricted due to existence of the preferable orientations of the indole ring. This assumption is confirmed by rather high anisotropy (0.159) of the Ac-18A-NH_2 Trp in the lipid environment. Specific orientation of the Trp residue relative to the lipid–water interface could arise from the orientational constraints experienced by Trp in the lipid phase and preferential orientation of the polypeptide chain. Thus, our finding suggesting that κ^2 values different from 0.67 can be considered as a consequence of the parallel with the membrane surface disposition of Ac-18A-NH_2 and decreased freedom of the Trp motion in the molecule of lipid-bound peptide. These results illustrate how RET studies can provide arguments in favor of specific orientation of the peptide relative to the membrane surface. However, such arguments can be obtained only in the case when non-random orientation of the lipid-bound peptide is combined with pronounced restriction of the Trp rotational mobility within the peptide molecule. For instance, in the case of 18A we failed to answer the question concerning the existence of the preferable peptide orientations because the x-intercept of the plots $d_c(\kappa^2)$ does not exclude the isotropic κ^2 value (Fig. 4b). The main reason for this seems to be a substan-

Table 2
Fluorescence anisotropy of the peptide tryptophan and fluorescent probes in the lipid-bound state

Ac-18A-NH_2 Trp	18A Trp	AV-PC	MBA	ANS
0.159 ± 0.004	0.068 ± 0.006	0.038 ± 0.004	0.046 ± 0.004	0.073 ± 0.007

tial freedom of the fluorophore motion since fluorescence anisotropy of the 18A Trp in the lipid environment is rather low (0.068) (Table 2).

In further considering the results of RET experiments we made an attempt to set the upper and lower κ^2 limits using the information on the fluorophore rotational mobility derived from the anisotropy measurements. Assuming that donor emission and acceptor absorption transition moments are axially distributed within a cone, dynamically averaged value of the orientation factor is given by [29]:

$$\kappa^2 = K^2 d_D d_A + 1/3(1 - d_D) + 1/3(1 - d_A) + \cos^2\theta_D d_D(1 - d_A) + \cos^2\theta_A d_A(1 - d_D) \quad (24)$$

$$K^2 = (\sin\theta_D \sin\theta_A \cos\Phi - 2\cos\theta_D \cos\theta_A)^2 \quad (25)$$

where θ_D and θ_A are the angles between the donor or acceptor cone axis and the translation vector connecting the oscillator centers; Φ is the angle between the planes containing the cone axes and translation vector; d_D and d_A are depolarization factors related to the steady-state (r) and fundamental (r_o) anisotropies of the donor and acceptor:

$$d_D = \left(\frac{r_D}{r_{oD}}\right)^{1/2}; \quad d_A = \left(\frac{r_A}{r_{oA}}\right)^{1/2} \quad (26)$$

In terms of the formalism developed by Dale et al. [29] the minimum (κ^2_{min}) and maximum (κ^2_{max}) κ^2 values are defined as:

$$\kappa^2_{min} = 2/3(1 - 0.5(d_D + d_A)) \quad (27)$$

$$\kappa^2_{max} = 2/3(1 + d_D + d_A + 3d_D d_A) \quad (28)$$

Presented in Table 3 are the orientation factor limits calculated from Eqs. (27) and (28) on the basis of anisotropy values measured for the peptide Trp and the acceptors employed (Table 2). The values of fundamental anisotropy were taken from the data reported earlier for anthrylvinyl fluorophore (0.08 at $\lambda_{ex} = 300$ nm [30]), MBA (0.34 at $\lambda_{ex} = 420$ nm [31]) and ANS (0.38 at $\lambda_{ex} = 360$ nm [32]). It is known that tryptophan absorbance in the range 250–300 nm is determined by the two electronic transitions ^1L_a and ^1L_b possessing orthogonally oriented transi-

Table 3
The limits of orientation factor and Trp distance from the lipid bilayer center

Donor	Acceptor	$\kappa_{min}{}^2$	$\kappa_{max}{}^2$	$d_{c\,min}$ (nm)	$d_{c\,max}$ (nm)
Ac-18A-NH_2 Trp	AV-PC	0.19	2.62	0	1.8
	MBA	0.30	1.93	0	1.8
	ANS	0.28	2.08	0	1.7
18A Trp	AV-PC	0.28	2.10	0.9	2.4
	MBA	0.38	1.58	1.3	2.4
	ANS	0.36	1.69	1.7	3.1

tion moments [33]. The excitation wavelength of 296 nm used in our experiments predominantly populates the ^1L_a state of the fluorophore whose transition moment lies in the plane of the indole ring [34]. Fundamental anisotropy for this state has been found to be 0.3 [1].

Estimation of the κ^2 bounds allowed us to determine the minimum ($d_{c\ min}$) and maximum ($d_{c\ max}$) Trp distances from the bilayer center by analyzing the plots d_c (κ^2) (Fig. 4). Comparison of the $d_{c\ min}$ and $d_{c\ max}$ values derived for various acceptors (Table 3) suggests the following limits of the possible Trp distances from the bilayer midplane: 1–1.8 nm for Ac-18A-NH_2 and 1.7–2.4 nm for 18A. As follows from the X-ray and neutron diffraction data, the distances from the membrane center falling in the range 1–1.8 nm cover the bilayer portion containing glycerol moiety, carbonyl and upper methylene groups of phospholipid molecules [35]. All these groups belong to the lipid–water interface that is thought to be preferable for the location of the peptide and protein tryptophan residues [36]. As indicated above, Trp residue of the peptides under study is situated at the polar helix side facing presumably hydrophilic bilayer region. Recent X-ray diffraction studies of Hristova et al. revealed that α-helix axis of Ac-18A-NH_2, lying parallel with the membrane surface, is located approximately 1.7 nm from the midplane of the model membranes composed of 1,2-dioleoyl-*sn*-glycero-3-phosphocholine, at the level of glycerol backbone marking the headgroup–hydrophobic core boundary [18]. In ideal cases such a helix position corresponds to the Trp location in the vicinity of phosphorylcholine moiety. However, because of dynamic nature of the membrane interface, conformational and orientational fluctuations of the peptide molecule, it seems likely that some residues from the polar helix surface could penetrate in the hydrophobic core, at the level of carbonyl groups or upper acyl chain carbons. Orientational fluctuations leading to increasing the depth of the Trp bilayer penetration can involve, in particular, rotation of the helix cylinder about the long axis and tilting motions of the peptide axis relative to the bilayer plane [37]. Molecular modeling of the Ac-18A-NH_2 conformations and orientations has shown that the most adequate description of the peptide in the DOPC bilayer environment is provided by the model of moderately disordered helix with the tilt angle fluctuating between 0 and 6° [18].

Our d_c estimates derived for Ac-18A-NH_2 do not exclude the possibility of the Trp penetration in the hydrophobic bilayer region. It is noteworthy in this context that, according to the results of parallax analysis [27], emission maximum (λ_{em}) of 333 nm observed in our study for Ac-18A-NH_2 corresponds to the Trp location in the non-polar microenvironment, at a distance of approximately 1 nm from the membrane center. In view of this it seems probable that association of Ac-18A-NH_2 with lipids causes the Trp residue to be located in the vicinity of carbonyls or initial carbons of the acyl chains. The validity of such an assumption is confirmed also by our findings indicating that efficiency of the fluorescence quenching by a polar quencher acrylamide undergoes approximately 10-fold decrease on the binding of Ac-18A-NH_2 to lipid vesicles.

The limits of the Trp distance from the membrane midplane recovered for 18A suggest that fluorophore can reside in the aqueous phase since $d_{c\ max}$ is greater than the half-width of the PC bilayer, being approximately 2.2 nm [37]. However, according to the literature [17] and our observations, the emission maximum of 18A exhibits a blue shift from 352 nm in buffer to 342 nm on the peptide binding to lipid vesicles. Such spectral effects are characteristic of the Trp penetration in the membrane interior. Given the details of the bilayer structure it can be assumed that the 18A Trp is located at the level of glycerol backbone ($d_c \sim 1.7$–1.8 nm) or phosphorylglycerol moiety ($d_c \sim 2$–2.2 nm [38]). This assumption is in accordance with the results of Clayton and Sawyer [17] indicating that the 18A Trp resides in the headgroup bilayer region. Analysis of the d_c limits and λ_{em} values of the peptides being examined strongly suggests that the Trp residue of Ac-18A-NH_2 penetrates deeper in the bilayer interior than that of 18A. This finding is consistent with the fact that the N- and C-terminal protection of 18A markedly increases its helicity and lipid affinity [14,15]. As follows from the

circular dichroism data [15], in the aqueous solution α-helix content of Ac-18A-NH_2 is ~ sevenfold higher than that of 18A, while in the lipid phase blocked 18A has ~twofold greater helicity compared to the unblocked peptide. For this reason Ac-18A-NH_2 and 18A should markedly differ in the size of the helix non-polar face and, as a consequence, in the disposition of polypeptide chain within the membrane interior. Due to the greater hydrophobic area amphiphilic helix of Ac-18A-NH_2 appears to insert deeper in the lipid bilayer than that of 18A. This could be the simplest explanation for the recovered in our study difference between Ac-18A-NH_2 and 18A in the depth of Trp bilayer penetration.

In conclusion, the results of the present work can be summarized as follows. Examination of the resonance energy transfer between peptide Trp as a donor and AV-PC, MBA and ANS as acceptors has revealed some structural details of the model systems containing Ac-18A-NH_2 or 18A and PC vesicles. For extracting most adequate quantitative information from the RET data the model of energy transfer in the membrane systems proposed by Wolber and Hudson has been modified by considering the donor and acceptor planar arrays located at different levels within the bilayer interior. It has been demonstrated that uncertainty in the distance estimation originating from the unknown orientation factor can be reduced not only by the narrowing of κ^2 bounds on the basis of anisotropy measurements, but also by comparing the estimates derived for the widest possible set of acceptors. Based on such an approach the limits of the Trp distance from the bilayer center have been estimated to be 1–1.8 nm for Ac-18A-NH_2 and 1.7–2.4 nm for 18A. The applicability of the RET method to distinguishing between random and specific peptide orientations relative to the lipid–water interface has been confirmed by the findings obtained for Ac-18A-NH_2 which is known to orient parallel with the membrane surface. In this case the range of orientation factor values derived from the data fitting has been found not to include the isotropic value corresponding to the random reorientation of donor and acceptor.

Acknowledgements

This work was supported in part by grants from the Research Fellowship of the Japan Society for the Promotion of Science (RC 30026103 for G.G. and 12470488 for T.H.) We are indebted to referees for their valuable remarks.

References

[1] J.R. Lakowicz, Principles of Fluorescent Spectroscopy, New York, Plenum Press, 1999.
[2] J. Matko, M. Edidin, Energy transfer methods in detecting molecular clusters on cell surfaces, Meth. Enzymol. 278 (1997) 444–462.
[3] L. Loura, A. Fedorov, M. Prieto, Partition of membrane probes in a gel/fluid two-component lipid system: a fluorescence resonance energy transfer study, Biochim. Biophys. Acta 1467 (2000) 101–112.
[4] J. Silvius, M. Zuckermann, Interbilayer transfer of phospholipid-anchored macromolecules via monomer diffusion, Biochemistry 32 (1993) 3153–3161.
[5] P. Wu, L. Brand, Resonance energy transfer: methods and applications, Anal. Biochem. 218 (1994) 1–13.
[6] M. Soekarjo, M. Eisenhawer, A. Kuhn, H. Vogel, Thermodynamics of the membrane insertion process of the M13 procoat protein, a lipid bilayer traversing protein containing a leader sequence, Biochemistry 35 (1996) 1232–1241.
[7] T. Dewey, G. Hammes, Calculation of fluorescence resonance energy transfer on surfaces, Biophys. J. 32 (1980) 1023–1036.
[8] B. Snyder, E. Freire, Fluorescence energy transfer in two dimensions. A numeric solution for random and nonrandom distributions, Biophys. J. 40 (1982) 137–148.
[9] M. Doody, L. Sklar, H. Pownall, J. Sparrow, A. Gotto, L. Smith, A simplified approach to resonance energy transfer in membranes, lipoproteins and spatially restricted systems, Biophys. Chem. 17 (1983) 139–152.
[10] P. Wolber, B. Hudson, An analytic solution to the Forster energy transfer problem in two dimensions, Biophys. J. 28 (1979) 197–210.
[11] P. Wu, L. Brand, Orientation factor in steady state and time-resolved resonance energy transfer measurements, Biochemistry 31 (1992) 7939–7947.
[12] P. Spuhler, G. Anantharamaiah, J. Segrest, J. Seelig, Binding of apolipoprotein A–I model peptides to lipid bilayers. Measurement of binding isotherms and peptide–lipid headgroup interactions, J. Biol. Chem. 269 (1994) 23904–23910.
[13] V. Mishra, M. Palgunachari, Interaction of model class A1, class A2 and class Y amphipathic helical peptides with membranes, Biochemistry 35 (1996) 11210–11220.
[14] Y. Venkatachalapathi, M. Phillips, R.M. Epand, R.F. Epand, E. Tytler, E. Segrest, G. Anantharamaiah, Effect

of end group blockage on the properties of a class A amphipathic helical peptides, Proteins: Struct, Funct. Genet. 15 (1993) 349–359.
[15] V. Mishra, M. Palgunachari, J. Segrest, G. Anantharamaiah, Interactions of synthetic peptide analogs of the class A amphipathic helix with lipids, J. Biol. Chem. 26 (1994) 7185–7191.
[16] J. Segrest, H. Deloof, J. Dohlman, C. Brouilette, G. Anantharamaiah, Amphipathic helix motif-classes and properties, Proteins: Struct., Funct. Genet. 8 (1990) 103–117.
[17] A. Clayton, W. Sawyer, The structure and orientation of class A amphipathic peptides on a phospholipid bilayer surface, Eur. Biophys. J. 28 (1999) 133–141.
[18] K. Hristova, W. Wimley, V. Mishra, G. Anantharamaiah, J. Segrest, S. White, An amphipathic α-helix at a membrane interface: a structural study using a novel X-ray diffraction method, J. Mol. Biol. 290 (1999) 99–117.
[19] G. Gorbenko, Resonance energy transfer study of hemoglobin and cytochrome c complexes with lipids, Biochim. Biophys. Acta 1409 (1998) 12–24.
[20] G. Gorbenko, Structure of cytochrome *c* complexes with phospholipids as revealed by resonance energy transfer, Biochim. Biophys. Acta 1420 (1999) 1–13.
[21] J. Molotkovsky, P. Dmitriev, L. Nikulina, L. Bergelson, Synthesis of new fluorescence labeled phosphatidylcholines, Bioorg. Khim. 5 (1979) 588–594.
[22] G. Bartlett, Phosphorus assay in column chromatography, J. Biol. Chem. 234 (1959) 466–468.
[23] E. Kirby, R. Steiner, The influence of solvent and temperature upon the fluorescence of indole derivatives, J. Phys. Chem. 74 (1970) 4480–4490.
[24] A. Lee, J. Rogers, D. Wilton, K. Ghiggino, D. Phillips, Spectroscopic resolution of drug binding sites in biological membranes, FEBS Lett. 94 (1978) 171–174.
[25] G.E. Dobretsov, Fluorescent Probes in the Studies of Cells, Membranes and Lipoproteins, Nauka, Moscow, 1989.
[26] V.G. Ivkov, G.N. Berestovsky, Dynamic Structure of Lipid Bilayer, Nauka, Moscow, 1981.
[27] J. Ren, S. Lew, Z. Wang, E. London, Transmembrane orientation of hydrophobic α-helices is regulated both by the relationship of helix length to bilayer thickness and by the cholesterol concentration, Biochemistry 36 (1997) 10213–10220.
[28] S. Lund-Katz, M. Phillips, V. Mishra, J. Segrest, G. Anantharamaiah, Microenvironments of basic amino acids in amphipathic α-helices bound to phospholipid: C NMR studies using selectively labeled peptides, Biochemistry 34 (1995) 9219–9226.
[29] R. Dale, J. Eisinger, W. Blumberg, The orientational freedom of molecular probes. The orientation factor in intramolecular energy transfer, Biophys. J. 26 (1979) 161–194.
[30] L. Johansson, J. Molotkovsky, L. Bergelson, Fluorescence properties of anthrylvinyl lipid probes, Chem. Phys. Lipids 53 (1990) 185–189.
[31] G. Dobretsov, V. Petrov, V. Mishiev, G. Klebanov, Yu. Vladimirov, 4-Dimethylamino-chalkon and 3-methoxybenzanthrone as fluorescent probes to study biomembranes, Studia Biophys. 65 (1977) 91–98.
[32] S. Anderson, G. Weber, Fluorescence polarization of the complexes of 1-anilino-8-naphthalenesulfonate with bovine serum albumin. Evidence for preferential orientation of the ligand, Biochemistry 8 (1969) 371–377.
[33] B. Valeur, G. Weber, Resolution of the fluorescence excitation spectrum of indole into ^1L_a and ^1L_b excitation bands, Photochem. Photobiol. 25 (1977) 441–444.
[34] B. Albinsson, M. Kubista, B. Norden, E. Thulstrup, Near-ultraviolet electronic transitions of the tryptophan fluorophore: linear dichroism, fluorescence anisotropy, and magnetic circular dichroism spectra of some indole derivatives, J. Phys. Chem. 93 (1989) 6646–6654.
[35] M. Wiener, S. White, Structure of a fluid dioleoylphosphatidylcholine bilayer determined by joint refinement of X-ray and neutron diffraction data, Biophys. J. 61 (1992) 434–447.
[36] W. Yau, W. Wimley, K. Gawrisch, S. White, The preference of tryptophan for membrane interfaces, Biochemistry 37 (1998) 14713–14718.
[37] A. Clayton, W. Sawyer, Site-specific tryptophan dynamics in class A amphipathic helical peptides at a phospholipid bilayer interface, Biophys. J. 79 (2000) 1066–1073.
[38] M. Caffrey, G. Feigenson, Fluorescence quenching in model membranes. 3. Relationship between calcium adenosintriphosphatase enzyme activity and the affinity of the protein for phosphatidylcholines with different acyl chain characteristics, Biochemistry 20 (1981) 1949–1961.